

VARIABILITY OF ACTIVE GALACTIC NUCLEI

WOLFRAM KOLLATSCHNY , MARTIN W. OCHMANN  and MALTE A. PROBST 

*Institut für Astrophysik und Geophysik, Universität Göttingen,
Friedrich-Hund Platz 1, 37077 Göttingen, Germany
E-mail: wkollat@gwdg.de*

Abstract. All active galactic nuclei (Seyfert 1 galaxies, quasars) are variable in the continuum flux. Furthermore, their broad emission lines vary as well on time scales of weeks to years. First, we will present the results of variability campaigns on two prototype AGN. Then we will show what we can learn from the variability about the geometry and kinematics in the innermost regions that are surrounding the central supermassive black holes. The second part is dedicated to galaxies that show extreme variations in their spectral profiles - the so-called changing look AGN.

1. INTRODUCTION

Active galactic nuclei (AGN) exhibit flux variations in all frequencies on time scales of hours to decades. Typical rms variations in the optical continuum are on the order of 5 to 20 percent. As an example we show in Fig. 1 the continuum light curve of the Kepler AGN KIC 2694186 based on observations taken with the Kepler satellite for the years 2011 - 2014 (Smith et al. 2018). Occasionally, changes of up to a factor of 2 are observed in the optical luminosity. These continuum variations are often accompanied by intensity and profile variations in the broad emission lines. We present in Fig. 2 optical spectra of the highly variable Seyfert galaxy Mrk110 over a period of four years (Bischoff & Kollatschny 1999).

The study of the variable line intensities and line profiles – in comparison to the continuum variations – provides information about the structure and kinematics of the line-emitting Broad Line Region (BLR) in AGN. Variability campaigns of AGN over periods of many months have been carried out for more than 100 Seyfert galaxies up to now (e.g. Peterson et al. 2002; Bentz et al. 2013, Shapovalova et al. 2013). However, detailed velocity-resolved reverberation mapping studies have been performed for only a few dozen objects.

2. SPECTRAL VARIABILITY IN AGN

In this chapter I will concentrate on the results of two variable AGN: The narrow-line Seyfert 1 galaxy Mrk 110 and the prototype AGN NGC 5548.

A detailed variability campaign of Mrk 110 has been performed with the 9.2-m Hobby-Eberly Telescope (HET) at McDonald Observatory over a period of 7 months. Kollatschny et al. (2001) show in Fig. 3 the individual spectra of the campaign as well as their mean and rms spectra. The rms spectrum illustrates the continuum and line profile variations. Therefore, the constant narrow components disappear. Considering the delays of the emission lines with respect to the continuum variations, they were

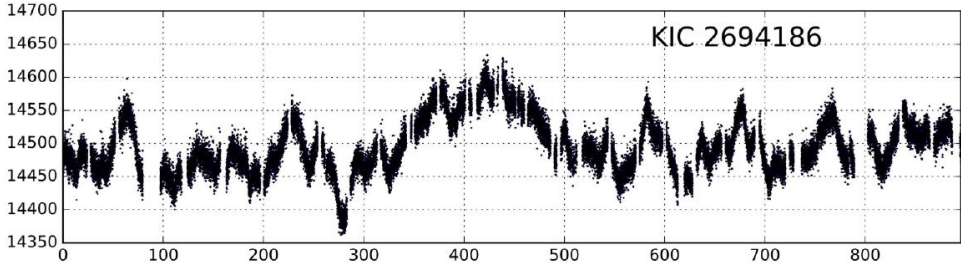


Figure 1: Light curve of the Kepler AGN KIC 2694186 from 2011 - 2014 (flux in units of counts s^{-1} and time in rest-frame days). (Smith 2018)

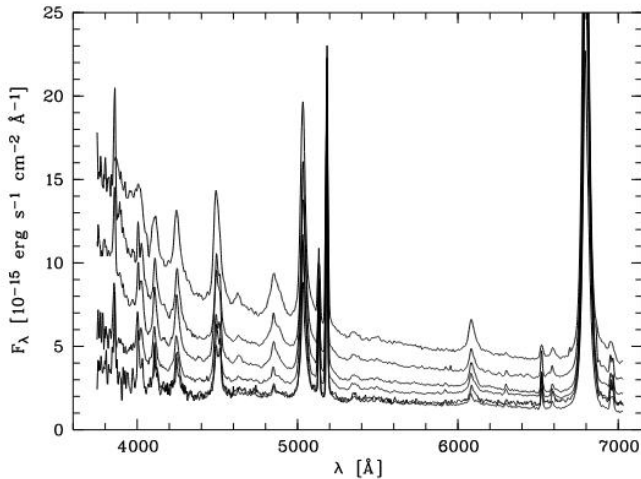


Figure 2: Normalized spectra of Mrk110 taken at different epochs in 1988 Oct., 1889 Oct., 1988 March, 1989 Feb., 1989 May, 1992, Jan. (from bottom to top) (Bischoff et al., 1999).

able to verify an ionization stratification of the BLR. The integrated Balmer and helium (He I, II) emission lines are delayed by 33 and 3 light days relative to the optical continuum variations respectively. A virial mass of $M = 1.8 \times 10^7 M_{\odot}$ for the central black hole has been derived from the radial distances of the different emission lines and from their widths. Furthermore, we calculated 2-D $\text{CCF}(\tau, v)$'s, i.e. the velocity-resolved correlation of the segmented broad-line profile and the continuum light curve (e.g. $\text{H}\beta$, Fig. 4, Kollatschny 2003). The outer wings of the line profiles respond much faster to continuum variations than the central regions. The comparison of the observed profile variations with model calculations of different velocity fields (e.g. Welsh & Horne 1991) indicates an accretion disk structure of the broad-line emitting region in Mrk 110. Comparing the velocity-delay maps of the different emission lines with each other indicates a clear radial stratification in the BLR. Furthermore, the delays of the red line wings are slightly shorter than those of the blue wings. This points to an accretion disk wind in the BLR of Mrk 110.

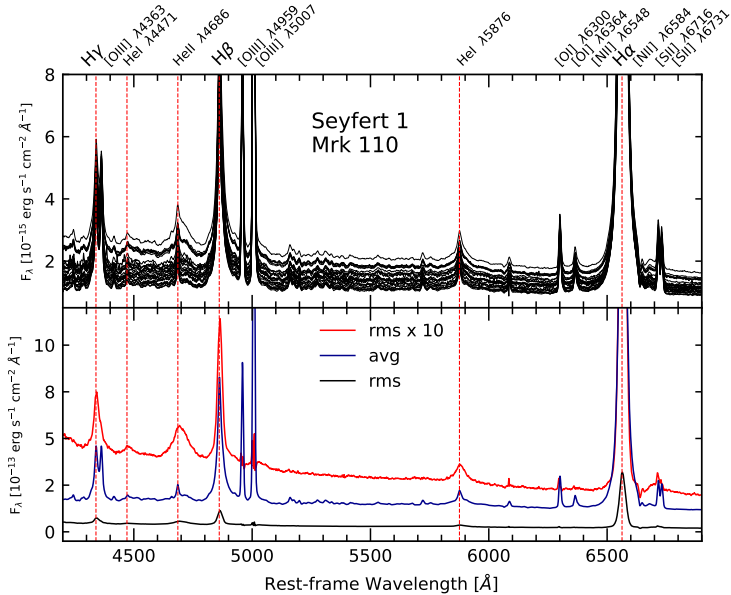


Figure 3: Spectra of Mrk110 taken with the Hobby Eberly Telescope in the years 1999 - 2000 (top). Their average and rms spectra are presented at the bottom. (Kollatschny et al. 2001)[adopted from M.W. Ochmann, PhD Thesis, 2023].

NGC 5548 is the best investigated variable AGN. De Rosa et al. (2015) carried out a six-month long reverberation mapping campaign on the Seyfert 1 galaxy NGC 5548 with the Hubble Space Telescope in 2014. Fig. 5 shows the light curves of the UV continuum and of the broad UV emission lines. The variations of all these emission lines lag behind those of the continuum: He II $\lambda 1640$ lags behind the continuum by $\simeq 2.5$ days only. Ly α $\lambda 1215$, C IV $\lambda 1550$, and Si IV $\lambda 1400$ lag the continuum by $\simeq 5$ –6 days. First velocity-resolved cross-correlation studies show a coherent structure of lag versus line-of-sight velocity for the emission lines: the outer wings of the broad UV lines respond faster to continuum variations than the line cores. Again, this indicates higher-velocity broad-line-region clouds at smaller distances from the center.

The two-dimensional wavelength–delay maps of the UV emission lines are presented in Fig. 5 (Horne et al. 2021). The virial envelopes enclosing the emission-line responses indicate that the reverberating gas is bound to the black hole. The stratified ionization structure is evident. The He II response within 5–10 lt-days has a broad single-peaked velocity profile. The Ly α and C IV responses extend from inside 2 to outside 20 lt-days, with double peaks at ± 2500 km s $^{-1}$ in the 10–20 lt-day delay range. Horne et al. (2021) interpret the maps in terms of a Keplerian disk with an outer rim at $R = 20$ lt-days. They derive a central black hole mass of $M = 7 \times 10^7 M_{\odot}$ in NGC 5548.

3. CHANGING-LOOK AGN

Optical/UV changing-look AGN exhibit transitions from spectral type 1 to spectral type 2 and vice versa. In this case, the optical spectral classification can change as a result of a variation in the accretion rate, accretion disk instabilities, or a variation

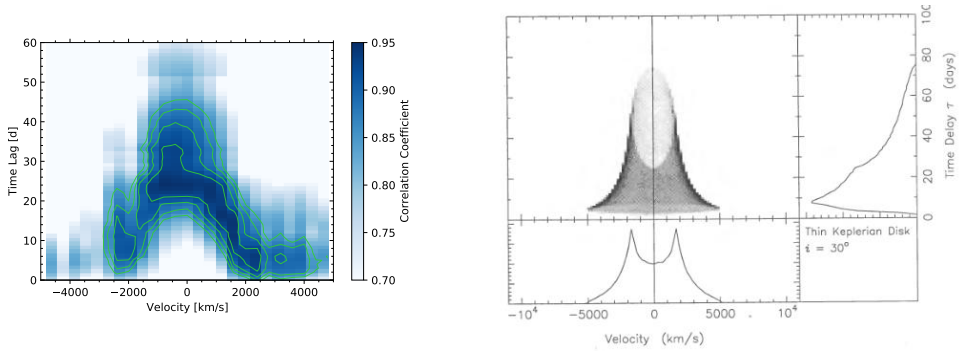


Figure 4: Left: The 2-D CCF(τ, v) shows the correlation of the H β line segment light curves with the continuum light curve as a function of velocity and time delay. Contours of the correlation coefficient are overplotted at levels between 0.800 and 0.925 (solid lines) (Kollatschny 2003) [adopted from M.W. Ochmann, PhD Thesis, 2023]. Right: Theoretical two dimensional transfer function (echo image) for a thin Keplerian disk BLR model viewed at an inclination of 30 degree (Welsh & Horne 1991).

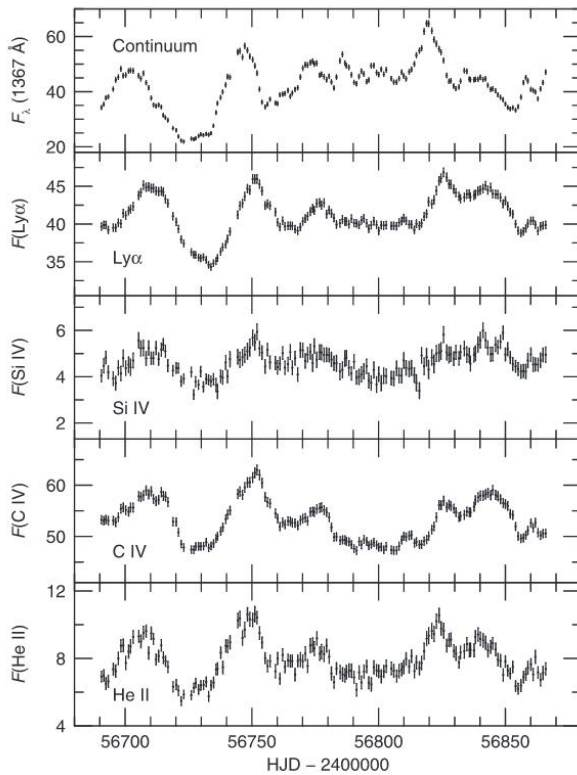


Figure 5: Continuum and integrated line light curves based on the HST variability campaign of NGC5548 in 2014 (De Rosa 2015)

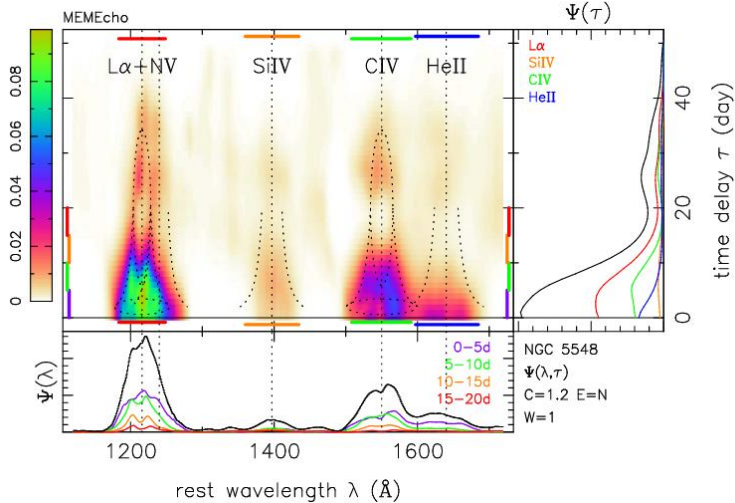


Figure 6: Two-dimensional wavelength–delay map reconstructed from the MEMECHO fit to the UV spectra from HST. Delays are measured relative to the UV continuum light curve. The ellipses shown for Ly α and C IV correspond to Keplerian disk orbits at $R = 2$ and 20 lt-days (Horne et al. 2021).

in reddening. By analogy, AGN that show X-ray flux variations in combination with X-ray spectral variations, that is when a Compton-thick AGN becomes Compton-thin and vice versa, are called changing-look AGN. In extreme cases, AGN have shown variability amplitudes by a factor of more than 20 in the X-ray regime.

We show in Fig. 7 the decreasing optical continuum flux in the Seyfert galaxy Fairall 9 for the years from 1978 until 1984 (Kollatschny & Fricke 1985). The continuum flux was equivalent to that of a quasar in 1978. The flux faded continuously to 20 percent of its original flux value within 6 years.

The Balmer and Helium lines weakened by a factor of more than 6 for the final 3 years from 1981 to 1984. The spectrum of Fairall 9 was approaching that of a Seyfert 2 type in 1984 (see Fig. 7).

Trakhtenbrot et al. (2019) studied the sudden optical and ultraviolet (UV) brightening of 1ES 1927+654, previously known as a narrow-line active galactic nucleus. 1ES 1927+654 was part of the small and peculiar class of “true Type-2” AGNs that lack broad emission lines and line-of-sight obscuration. Trakhtenbrot et al. (2019) carried out a high-cadence spectroscopic monitoring: they captured the appearance of a blue, featureless continuum, followed several weeks later by the appearance of broad Balmer emission lines (see Fig. 8). This timescale was generally consistent with the expected light travel time between the central engine and the broad line emission region in broad-line AGN. The nature and timescales of the photometric and spectral evolution disfavored both a change in line-of-sight obscuration and a change in the overall rate of gas inflow as driving the drastic spectral transformations seen in this AGN. Although the peak luminosity and timescales were consistent with those of tidal disruption events seen in inactive galaxies, the spectral properties were not. The X-ray emission displayed a markedly different behavior, with frequent flares on timescales of hours to days.

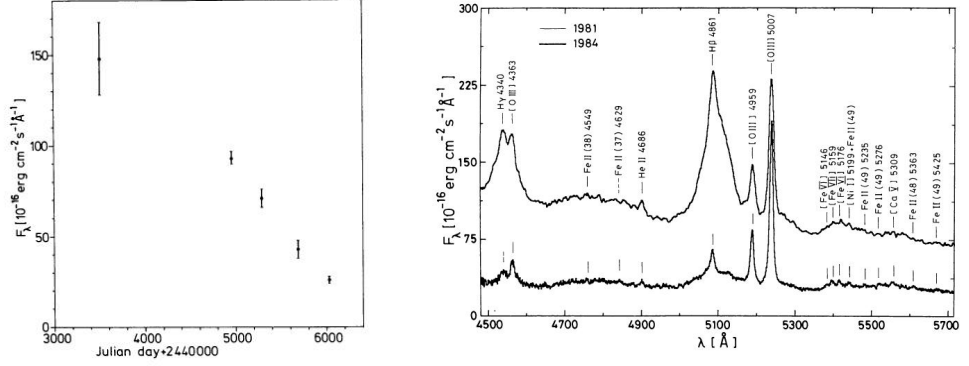


Figure 7: Left: Optical continuum decreasing flux in Fairall 9 from 1978 until 1984. Right: Fairall 9 spectra from 1981 and 1984

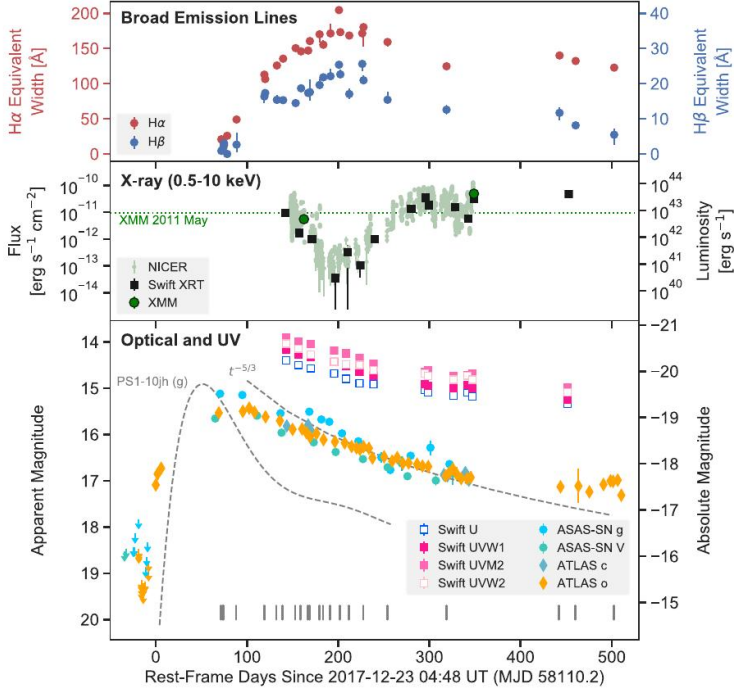


Figure 8: Light curve and equivalent-width evolution of 1ES 1927+654 during the flare. Top: equivalent-width evolution of the broad components of the $H\beta$ and $H\alpha$ emission lines (Trakhtenbrot 2019). Middle: X-ray light curve obtained with Swift/XRT, NICER, and XMM-Newton. Bottom: optical and UV light curves, obtained with ATLAS, ASAS-SN, and Swift/UVOT.

NGC 3516 is another example of a changing-look AGN (e.g. Popović *et al.* 2023). They analyzed the $H\beta$ line profile variability over a period of 25 years from 1996 to 2021. They found that the transition from a Seyfert type 1 to a Seyfert type 2 is more connected to intrinsic effects than to an outer obscuring region.

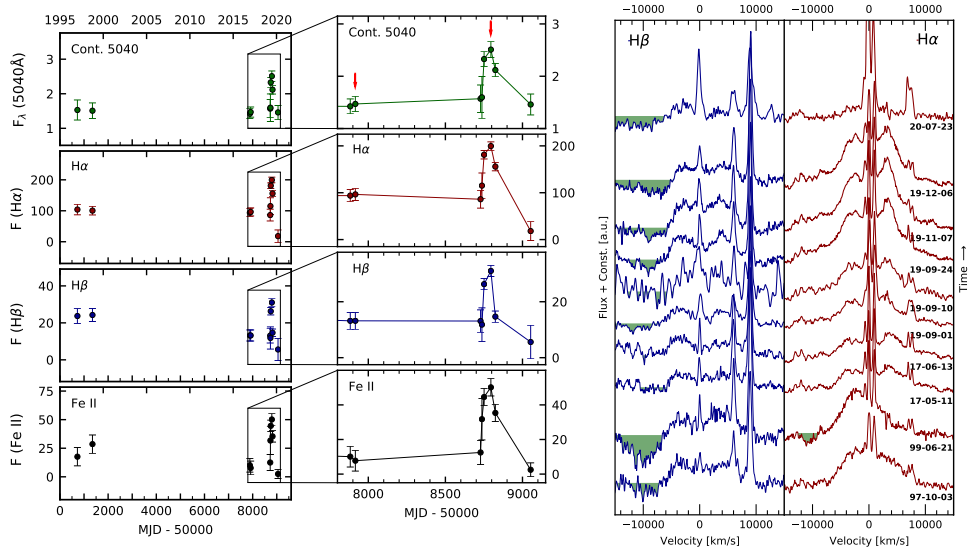


Figure 9: Left: Long-term light curves of the continuum flux density at 5040 \AA (in units of $10^{-15} \text{ ergs}^{-1} \text{ cm}^{-2} \text{ \AA}^{-1}$), as well as of the line fluxes of $H\alpha$, $H\beta$, and $\text{FeII}(42,48,49)$ (in units $10^{-15} \text{ ergs}^{-1} \text{ cm}^{-2}$) for the years 1997 until 2020. The right panel shows, in addition to the observations from 2017 and 2020 the variations in 2019 in more detail. The epochs of deep XMM-Newton observations are indicated by a red arrow.

Right: Line profiles of $H\alpha$ and $H\beta$ in velocity space after subtraction of the host galaxy spectrum. Absorption components in the blue wing of the Balmer lines (i.e. flux below zero) are shaded in green.

IRAS 23226-3843 has previously been classified as a changing-look candidate based on the comparison of optical spectra taken in the 1990s and optical as well as X-ray data (Swift, XMM-Newton, and NuSTAR) taken after a very strong X-ray decline in 2017 (Kollatschny et al. 2020). In 2019, Swift observations revealed a strong rebrightening in X-ray and UV fluxes. We aimed to study this outburst in greater detail in the optical and X-ray with SWIFT. We took optical follow-up observations of IRAS 23226-3843 from 2019 until 2021. The optical spectra have been secured with the SALT telescope as well as with the SAAO 1.9m telescope (Kollatschny et al. 2023).

IRAS 23226-3843 showed a strong optical and X-ray outburst in 2019 : The flux of the optical continuum varied by a factor of 1.6 within two months. This corresponds to a factor of 3 after correction for the host galaxy contribution. The X-ray continuum varied by a factor of 5.

The Balmer and FeII emission-line intensities showed comparable variability amplitudes during the outburst (Fig. 9). The $H\alpha$ emission-line profile of IRAS 23226-3843 had changed from a blue-peaked profile in the years 1997 and 1999 to a broad double-peaked profile in 2017 and 2019 (Fig. 9). However, there were no major profile variations during the transient event in 2019 despite the strong intensity vari-

ations. The double peaked Balmer lines were extremely broad. In addition, IRAS 23226-3843 exhibits strong FeII blends. This is in contrast to what is expected from Eigenvector 1 studies (Boroson & Green 1992). One year after the outburst, IRAS 23226-3843 changed its optical spectral type again and became a Seyfert type 2 object in 2020. Throughout all observations, blue outflow components are present in the optical Balmer lines and in the Fe band in the X-rays. Further, a deep broadband XMM/NuSTAR spectrum was taken during IRAS 23226-3843's maximum state in 2019. This spectrum is qualitatively very similar to a spectrum taken in 2017, but by a factor of 10 higher. The soft X-ray band appears to be featureless. The changing-look character of IRAS 23226-3843 is most probably caused by changes in the accretion rate - based on the short-term variations on timescales of weeks to months.

4. SUMMARY

The study of variable AGN is an active field of research for more than 40 years. It will receive an additional push when the Large Synoptic Survey Telescope (LSST) will become operational in 2024.

Acknowledgements

The authors greatly acknowledge the support by the DFG grant KO 857/35-1 and the support of the German Aerospace Center (DLR) within the framework of the 'Verbundforschung Astronomie und Astrophysik' through grant 50OR230.

References

- Bentz, B.C., Denney, K.D., Grier, C.J. et al.: 2013, *The Astrophysical Journal*, **767**, 149.
Bischoff, K., Kollatschny, W.: 1999, *Astron.Astrophys.*, **345**, 49.
Boroson, T.A., Green, R.F.: 1992, *The Astrophysical Journal Suppl.*, **80**, 109.
De Rosa, M., Peterson, B.M., Ely, J. et al.: 2015, *The Astrophysical Journal*, **806**, 128.
Horne, K., De Rosa, M., Peterson, B.M. et al.: 2021, *The Astrophysical Journal*, **907**, 76.
Kollatschny, W.: 2003, *Astron.Astrophys.*, **407**, 461.
Kollatschny, W., Bischoff, K., Robinson, R., et al.: 2001, *Astron.Astrophys.*, **379**, 125.
Kollatschny, W., Fricke, K.: 1985, *Astron.Astrophys.Letters*, **146**, L11.
Kollatschny, W., Grupe, D., Parker, M. L., et al.: 2020, *Astron.Astrophys.*, **638**, A91.
Kollatschny, W., Grupe, D., Parker, M. L., et al.: 2023, *Astron.Astrophys.*, **670**, 103K.
Peterson, B.M., Berlind, P., Bertram, R. et al.: 2002, *The Astrophysical Journal*, **581**, 197.
Popović, L.Č., Ilić, D., Burenkov, A.N., et al.: 2023, *Astron.Astrophys.*, **675**, 178.
Shapovalova, A.I., Popović, L.Č., Burenkov, A.N. et al.: 2013, *Astron.Astrophys.*, **559**, A10.
Smith, K.L., Mushotzky R.F., Boyd, P.T. et al.: 2018, *The Astrophysical Journal*, **857**, 141.
Trakhtenbrot, B., Arcavi, I., MacLeod, C.L. et al.: 2019, *The Astrophysical Journal*, **883**, 94.
Welsh, W., Horne, K.: 1991, *The Astrophysical Journal*, **379**, 586.